advances
in radiation oncology

Scientific Article

MDM2 Inhibition in a Subset of Sarcoma Cell Lines Increases Susceptibility to Radiation Therapy by Inducing Senescence in the Polyploid Cells

Samayita Das, PhD*

Innere Klinik (Tumorforschung), West German Cancer Center (WTZ), University Hospital Essen, University of Duisburg-Essen, Essen, Germany

Abstract

Purpose: Inhibition of p53 by amplification of MDM2 is one of the key contributors in the oncogenesis of a subset of soft tissue sarcoma (STS) known as well-/dedifferentiated liposarcoma. A small molecule MDM2 antagonist, nutlin-3, induces the p53 pathway by disrupting the interaction between MDM2 and p53. Radiation therapy is an integral component for treating liposarcoma and induces p53. Based on wild-type *TP53* status in liposarcoma, it was investigated whether MDM2 inhibition with irradiation led to enhanced reactivation of p53 and subsequent p53-mediated effects in liposarcoma.

Methods and Materials: Clonogenic assays, immunoblotting, flow cytometry/fluorescence-activated cell sorting, and senescence assays were employed in liposarcoma cell lines after co-treatment with nutlin-3 and radiation.

Results: Upon treatment with nutlin-3, 2 of the well-/dedifferentiated liposarcoma (MDM2^{Amp}/TP53^{WT}) cell lines displayed radiosensitivity with sensitization enhancement ratio values of >1. In contrast, the cell line with mutant *TP53* showed sensitization enhancement ratio values of ~ 1. Immunoblotting revealed induced reactivation of the p53-MDM2-p21 signaling axis in response to combination therapy in all cell lines with wild-type *TP53*. Removal of MDM2 inhibitor (with or without radiation therapy) led to the emergence of ploidy-based heterogeneous subpopulations (4N and >4N) in *TP53* wild-type cells and not in *TP53* mutant cells. Immunoblotting of cell cycle markers (G1, G2/M) revealed the generation of 4N G1 cells. Sorting and long-term fate analysis of different populations (2N, 4N, and >4N) by colony assay displayed attenuated colony-forming potential and augmented senescence of the 4N and >4N cells contributing to the radiosensitization effect.

Conclusions: Nutlin-3 increases the vulnerability of liposarcoma cell lines to radiation by augmented activation of p53. The cells underwent senescence. Presence and activation of p53 are required for exertion of the radiosensitizing effect by nutlin-3, but this is not the sole determinant of the effect. This study opens avenues for the clinical translation in a stratified group of patients with liposarcoma.

Introduction

TP53 has long been known as a tumor suppressor and the guardian of the genome and responds to diverse stress stimuli by orchestrating specific cellular responses such as transient cell cycle arrest and senescence.[1] Inactivating mutations are reportedly known to be among the most frequent genetic abnormalities in cancer.[2,3] Certain cancers harbor wild-type *TP53*, which is functionally silent by the amplification of *MDM2* (mouse double minute 2 homolog).[4,5] MDM2 suppresses p53 wild-type functions[6] by inhibiting transcriptional activity,[7] degradation of p53 by ubiquitin ligase activity,[8] and exporting p53 from the nucleus.[9] Examples are well-differentiated liposarcoma (WDLP) and dedifferentiated liposarcoma (DDLP), a subtype of soft tissue.[10,11] Both of these subtypes harbor supernumerary rings or marker chromosomes containing the 12q13-15 amplicon where *MDM2* resides.[12] They display exceptionally high *MDM2* amplification frequency (>90%),[13,14] which makes this a clinically relevant diagnosis marker and target. In cancers with wild-type *TP53*, reactivating its wild-type function by small molecule antagonists, which disrupt the interaction of p53 and MDM2, has been an attractive strategy.[15,16] Radiation therapy (RT) is an integral component of treating liposarcoma, activates the p53 pathway, and executes its effect by cell cycle arrest, apoptosis, and senescence. In this study, it was explored whether application of MDM2 inhibitor enhances the vulnerability of the WDLP/DDLP to RT by reactivating the suppressed p53 in an enhanced way and whether p53 is the determinant for the therapy response.

Materials and Methods

Cell lines and reagents

Human WDLP/DDLP liposarcoma cell lines (LPS853, T778, T449, SW872) were obtained from the institutional repository and the American Type Culture Collection. All cell lines except SW872 were characterized for harboring amplified *MDM2* and *CDK4* by SNP-Chip. Cell lines were cultured in RPMI-1640/DMEM supplemented with 15% fetal bovine serum (Hyclone, Logan, UT), 1× penicillin-streptomycin-amphotericin B (Invitrogen, Carlsbad, CA), and 1× glutamax (Invitrogen) at 37°C in a humidified incubator with 95% air and 5% CO2. Nutlin-3 (racemic of nutlin-3a and its inactive enantiomer nutlin-3b) was purchased from Sigma Aldrich (St. Louis, MO).

Clonogenic assay

After serial dilution (400-2500), cells were plated into 6-well plates in 2 mL medium in triplicate. Cells were treated with 5 μM nutlin-3 and within 20 to 30 minutes were irradiated with increasing doses (0, 2, 4, and 6 Gy). Cells were incubated for 24 hours, and nutlin-3 was washed off and replaced with fresh growth medium. Cells were irradiated using a ^{137}Cs irradiator (J.L. Shepherd and Associates, San Fernando, CA) at room temperature. After treatment, cells were maintained for 12 to 18 days, depending on the growth rate of the cell lines, for colony formation. Cells were then fixed for 1 hour with 70% methanol/acetic acid and stained for 15 minutes with Crystal violet in methanol. After staining, colonies were counted by naked eye and under a microscope with a cut-off of 50 viable cells for scoring a colony. Survival fraction was calculated according to the following formula: survival fraction = number of colonies formed in test condition/(number of cells seeded × plating efficiency of the control group). The sensitization enhancement ratio (SER) was calculated as the dose (Gy) for radiation alone divided by the dose (Gy) for radiation plus drugs (normalized for drug toxicity) as determined at a surviving fraction of 0.1.

Western blotting

Preparation of protein lysates was carried out from cell line monolayers following the standard protocols.[17,18] Protein concentrations were measured by Bio-Rad Protein Assay (Bio-Rad Laboratories, Hercules, CA). Equal amounts of protein were loaded into each well and separated in a 4% to 12% gradient sodium dodecyl sulfate–polyacrylamide gel electrophoresis (SDS-PAGE) gel. After transfer, blots were incubated with specific primary antibodies overnight at 4°C and horseradish peroxidase (HRP)-conjugated secondary antibody for 2 hours. Chemiluminescence was captured and quantified using a FUJI LAS3000 system with Science Lab 2001 Image Gauge 4.0 software (Fujifilm Medial Systems, Stamford, CT).

Antibodies

Mouse p21 and β-actin antibodies were from Sigma. Cyclin D1 (H-295 rabbit) antibody was from Santa Cruz Biotechnology (Santa Cruz, CA). Mouse MDM2 antibody was from Zymed Laboratories (South San Francisco, CA). Antibodies against phospho p53 (Ser-15), p53, cyclin A, cyclin B, phospho H3 (Ser-10), and HRP-conjugated

secondary antibodies (antirabbit and antimouse) were purchased from Cell Signaling Technology (Beverly, MA).

Cell cycle analysis

Cells were seeded in 12-well plates, grown to 60% confluence, and then treated for 48 hours with DMSO, 5 µM nutlin-3, 4 Gy, or a combination of both. Flow cytometric measurement (FACS Celesta, BD Biosciences, San Jose, CA) was carried out after fixation and staining with Propidium Iodide (PI) (Beckman Dickinson, Heidelberg, Germany). Data analysis was performed using BD Biosciences Diva software.

Apoptosis assay

Luminescent Caspase Glo assay (Promega, Madison, WI) was used to detect cellular apoptosis, as represented by activation of caspase 3/7, according to the manufacturer's protocol. Luminescence was measured with a Genion luminometer (Tecan, Crailsheim, Germany). All measurements were carried out in triplicate wells. Average and standard deviation were calculated from the technical replicates.

Senescence assay

SA-β-galactosidase (β-gal) staining was performed using a β-Galactosidase Staining Kit (Cell Signaling Technology) at pH 6.0 following the manufacturer's protocol, and images were taken by bright field light microscope at 40× magnification.

MTT (3-(4, 5-dimethylthiazol-2-yl)-2, 5-diphenyl-2H-tetrazolium bromide) assay

For each experiment, the appropriate number of cells was plated (decided empirically) to be in their log phase of growth 24 hours later. After treatment and irradiation in the next day, they were kept for 6 days. Before the assay, media was removed. MTT (3-(4, 5-dimethylthiazol-2-yl)-2, 5-diphenyl-2H-tetrazolium bromide) reagent was prepared (0.5 mg/mL), and 100 µL was added to the cells and kept at 37°C for 4 to 5 hours until crystals were formed. The crystal was solubilized thoroughly by adding organic solvent. At the plate shaker, plates were shaken for 5 minutes, and absorption was measured at 560 nm with a Genion luminometer (Tecan, Crailsheim, Germany). Calculation was performed in the following way. The absorbance of the blank was subtracted from all samples. Absorbance values from the treated samples were divided or normalized by those of the control values and multiplied by 100 to obtain percentage of cell viability. Absorbance values lower than the control values suggest cell death or growth inhibition. Cell viability (%) = [(Treated$_{Abs}$ − Blank$_{Abs}$)/(Control$_{Abs}$ − Blank$_{Abs}$)] ×100.

Hoechst 33342 staining and live cell sorting

For live cell sorting, after trypsinization and centrifugation, 10^6 cells were stained with Hoechst 33342 (Sigma-Aldrich). Doublets were gated out by Forward Scatter-Area underneath the peak (FSC-A) versus Forward Scatter-Width (FSC-W) plotting. Cell sorting was performed based on the DNA content using a BD Biosciences (FACSvantage SE DIVA) cytometer equipped with aN ultraviolet excitation laser. Sorted cells were plated at low density for colony forming assays.

Statistics

For evaluating the significance between the groups, Student t test was used. A P value ≤.05 was considered significant. Data are mean ± standard deviation if not otherwise indicated.

Results

Radiosensitization of certain liposarcoma cells harboring amplified MDM2 and wild-type TP53 by MDM2 inhibition

To assess whether disruption of MDM2-p53 interaction by small-molecule inhibitor nutlin-3 augments vulnerability to RT, liposarcoma cell lines (Table 1) were treated with 5 µM nutlin-3 for 24 hours, increasing

Table 1   Liposarcoma cell lines

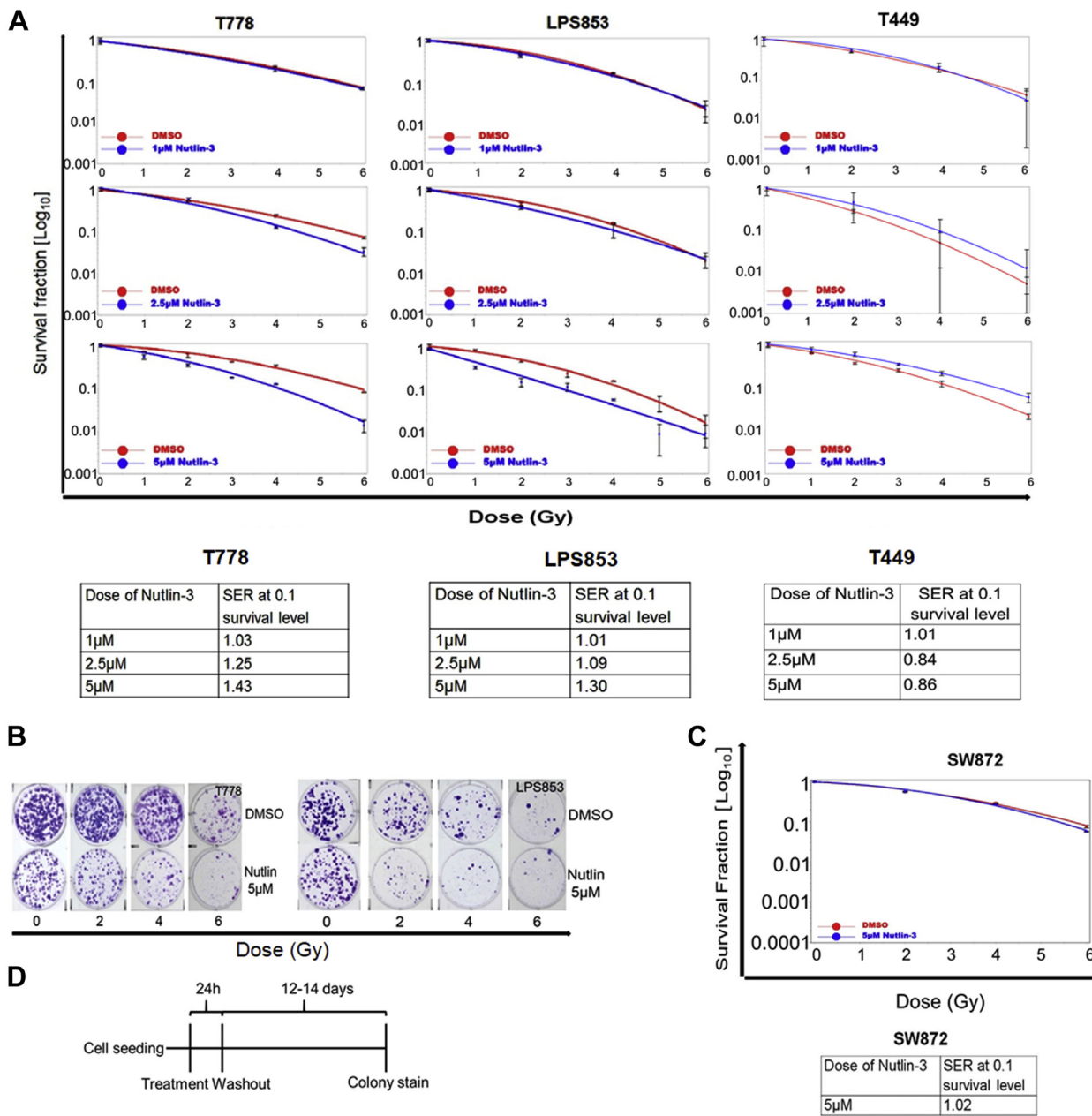| Cell line	Origin/histology	TP53 status	MDM2 copy no.
LPS853	Dedifferentiated	Wild-type	>10
T778	Well-differentiated	Wild-type	>20
T449	Well-differentiated	Wild-type	>20
SW872	Undifferentiated	Mutation (I251N)	∼2

Figure 1 Nutlin-3 mediated radiosensitization in liposarcoma cell lines. (A) Cell survival curves derived from clonogenic assays of 3 well-differentiated liposarcoma and dedifferentiated liposarcoma ($MDM2^{Amp}/TP53^{WT}$) cell lines (LPS853, T778, and T449) after treatment with increasing doses of nutlin-3 (1 μM, 2.5 μM, 5 μM) and increasing doses of radiation therapy (2 Gy, 4 Gy, and 6 Gy). Chart represents the sensitization enhancement ratio values at 0.1 survival fraction. (B) Representative images from the clonogenic assays for LPS853 and T778. (C) Cell survival curve derived from clonogenic assays of 1 undifferentiated liposarcoma ($TP53^{Mut}$) cell line (SW872) with 5 μM nutlin-3. Chart represents the sensitization enhancement ratio values at 0.1 survival fraction. (D) Schedule of treatment with nutlin-3 and radiation therapy.

doses of RT, or a combination of both (Fig 1). Radiosensitization was observed in 2 of the DDLPS ($MDM2^{Amp}/TP53^{WT}$) cell lines (T778 and LPS853), with a SER of 1.43 and 1.3, respectively, at 0.1 survival fraction (Fig 1A and 1B). As expected, SW872, which

harbors an inactivating p53-mutation, did not show radiosensitivity (Fig 1C) to MDM2 inhibition ($SER_{10} = 1.02$). However, T449 (Fig 1A) harboring amplified $MDM2$ and wild-type $TP53$ did not show radiosensitization ($SER_{10} = 0.86$).
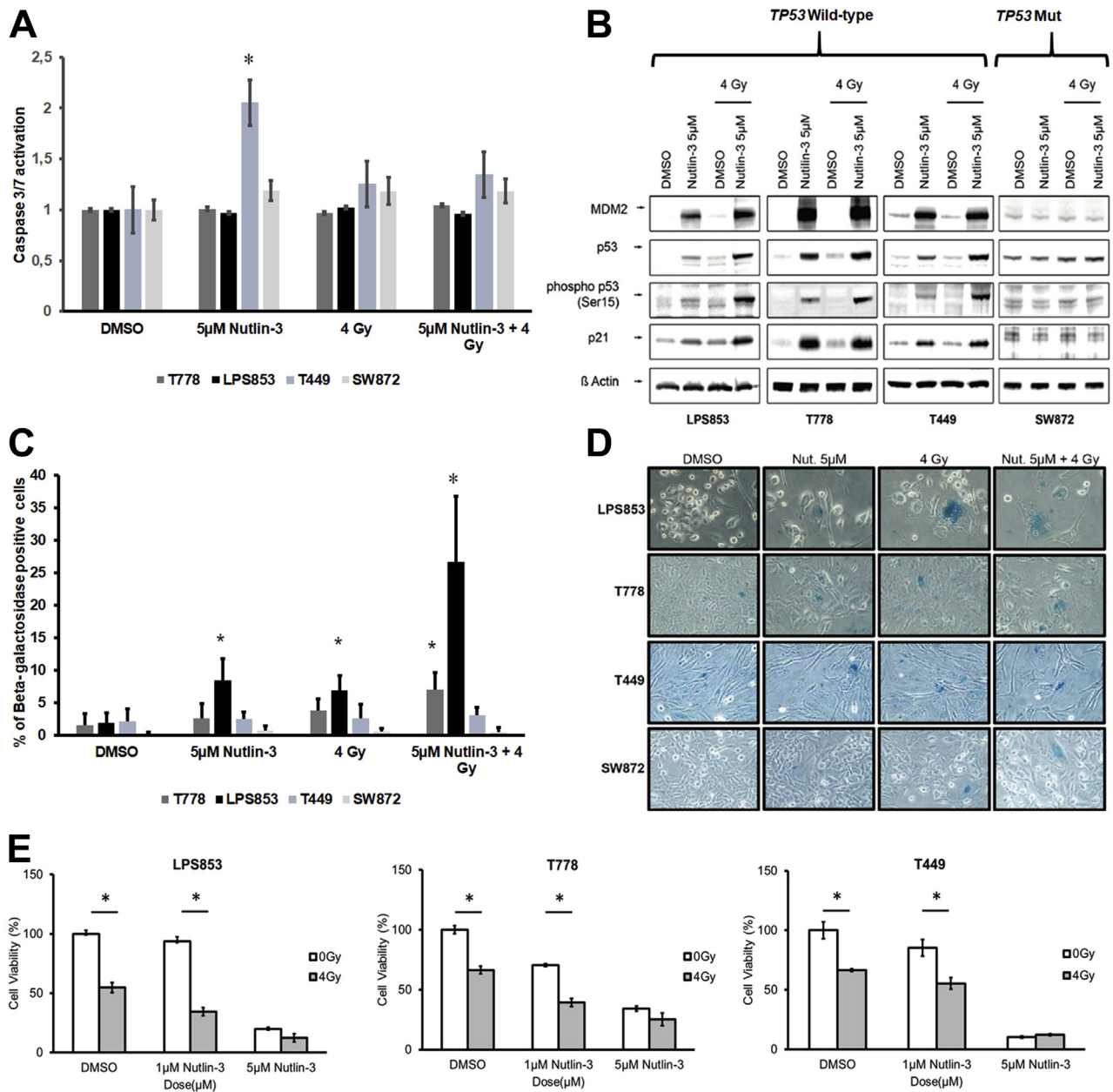
Figure 2 Therapy-driven cellular fates in liposarcoma. (A) Apoptotic response as measured by caspase 3/7 activation after 24 hours of treatment with DMSO or nutlin-3, irradiation, or a combination of both. (B) Immunoblot studies showing effects of nutlin-3 alone, radiation alone, or their combination on expression of MDM2, p53, phospho p53 (serine-15), p21 in liposarcoma cell lines cells 48 hours after treatment. (C) Quantification of senescence-associated β-galactosidase staining. The bar graphs represent mean percentage of β-galactosidase−positive cells. The error bars indicate standard deviation. (D) Corresponding bright field images from β-galactosidase stained cells. (E) Bar graphs represent normalized absorbance or percentage of cell viability of the liposarcoma cells (LPS853, T778, and T449) in response to increasing doses (1 μM, 5 μM) of nutlin-3, radiation therapy (4 Gy), and nutlin-3 plus radiation therapy treated for 192 hours (continuous treatment). *$P \leq .05$.

Induction of cell cycle arrest, senescence as short-term effect, and unperturbed apoptosis

Apoptosis measurement by caspase 3/7 assay indicated an unperturbed apoptotic response to the treatments in LPS853, T778, and SW872 (Fig 2A). Notably, nutlin-3 induced a ∼2-fold increase in caspase activation in

T449 ($P < .05$; Fig 2A), and in another DDLP, LPS141 (Fig E2A; available online at https://doi.org/10.1016/j.adro.2019.11.004) was further suppressed by the addition of RT.

For detection of senescence, β-gal staining and quantification were carried out after 48 hours of treatment. Nutlin-3 alone moderately induced

senescence (10% of β-gal positive cells) only in LPS853, which was increased ∼3-fold by addition of RT. In contrast, no significant induction of senescence was observed in T778, T449, and SW872 (Fig 2C and 2D). For determining the perturbation in intracellular signaling of the MDM2-p53-p21 axis in response to therapy, an immunoblotting analysis was carried out after 48 hours (Fig 2B). As expected, p53, MDM2, and p21 were upregulated in response to nutlin-3 and co-treatment in all cell lines except SW872. An enhanced phospho-p53 stabilization (phospho Ser-15) was detected in response to co-treatment in all cells with wild-type TP53.

To observe the cell viability in response to the treatments, the cell lines (LPS853, T778, T449) with wild-type TP53 were treated for 192 hours with increasing doses (1 μM and 5 μM) of nutlin-3 ± RT (4 Gy). For LPS853 and T778, the reduction in the cell viability in response to 5 μM nutlin-3, RT (4 Gy), and 5 μM nutlin-3 plus RT was 80%, 55%, 90% and 70%, 30%, 80%, respectively. In contrast, for T449, a dose-dependent decrease in the cell viability was observed for continuous treatment with nutlin-3 alone. However, the addition of RT did not exert an additive effect at the dose of 5 μM of nutlin-3 (Fig 2E). These results further support the clonogenic assay results.

Emergence of ploidy-based heterogeneity on drug removal and perturbation in the cell cycle proteins

Cell cycle analysis revealed enhanced G2 arrest (by increased 4N DNA content by PI stain) after 48 hours of treatment with nutlin-3 plus RT in LPS853 (76%) and T778 (57%; Fig 3A), compared with the respective monotherapies. In contrast, SW872 cells displayed an unperturbed cell cycle distribution in response to the treatments (Fig 3A) after 48 hours of treatment. Immunoblot studies for cell cycle–related markers (Fig 3C) after 48 hours of nutlin-3 treatment alone or in combination revealed reduction of cyclin B1 and cyclin A in all cells with wild-type TP53. Cyclin D1 was upregulated in LPS853 and T778, whereas histone H3 phosphorylation (Ser-10) was abrogated in all cells with wild-type TP53. The G1 marker was upregulated and G2/M markers were downregulated despite 4N DNA content, indicating the generation of 4N G1 cells. Cell cycle analysis was carried out after washout (Fig 3D, scheme 1 and scheme 2) after 48 hours for detection of the polyploid population. A marked increase of the >4N fraction in nutlin-3 plus RT–treated LPS853 (46% and 42%, respectively) and T778 (5% and 25%, respectively) was observed. In contrast, SW872 did not display therapy-driven polyploidy (Fig 3A and 3B).

Generation of the polyploid fraction upon drug removal was observed in T449 (Fig E1B; available online at https://doi.org/10.1016/j.adro.2019.11.004). Cell cycle proteins after 48 hours of treatment were differently regulated in T449. Cyclin D1 (Fig 3C) was observed to be overexpressed and unperturbed in response to the therapies in T449.

Senescence and attenuated clonal ability of >4N population led to ultimate effect in a subset of sarcoma harboring wild-type TP53

As depicted in Figure 3, treatment with nutlin-3 alone and even more pronouncedly in combination with RT resulted in an accumulation of >4N populations (ie, changing the clonal dynamics of the population after a 48-hour washout period; Fig 3D, scheme 2). Therefore, this study aimed to analyze the long-term fate of the ploidy-based variant populations by colony assay and senescence assay. To address that, therapy-generated ploidy-based variant populations were sorted after Hoechst 33342 staining (Fig 3D, scheme 1 and scheme 2), seeded at low cellular density (as single cells), and allowed to form colonies for 12 to 17 days.

The colony-forming abilities of the 2N population were higher compared with the 4N population in all treatment groups (5 μM nutlin-3 alone, 5 μM nutlin-3 plus RT for LPS853 and T778; P value ≤.05) with a nonsignificant trend in the RT alone group (LPS853; P = .44, T778; P = .08). The colony forming ability of the 4N populations was highly impaired in the nutlin-3 alone (LPS853 3% ± 0.4%, T778 5% ± 2%) and RT alone (LPS853 1.6% ± 1.6%, T778 5% ± 0.5%) groups and was further attenuated in combination treatment (LPS853 0.6% ± 0.7%, T778 0.9% ± 0.2%; Fig 4A).

For T778, >4N populations (Fig 3D, scheme 2) had attenuated clone-forming ability compared with 4N in response to the treatments (Fig 4A) with the most pronounced impairment in the combination treatment (4N 3.4% ± 0.2%, >4N 1.2% ± 0.2%, P ≤ .05). Induction of senescence in 2N and 4N (Fig 3D, scheme 1) was comparable to that in RT alone (2N 11.6% ± 2.34% vs 4N 11.98% ± 7.16%) and nutlin-3 alone (2N 5.5% ± 1.9% vs 4N 13.34% ± 11.66%) and significantly higher (P < .01) in the 4N population than in 2N in the nutlin-3 plus RT–treated group (2N 6.6% ± 3.1% vs 4N 53.93% ± 28.71%) in T778. Senescence for T778 cells (Fig 3D, scheme 2) was highest in 4N (68% ± 16.4%) and >4N (69.82% ± 17.91%) populations in response to the combined treatment (Fig 4B). For LPS853, the >4N population displayed a significantly lower colony forming potential than the 4N population in vehicle-treated (4N 3.7% ± 1.1%, >4N 0.3% ± 0.2%, P ≤ .05) and nutlin-3–treated (4N 3% ± 1%, >4N 0.6% ± 0.3%, P ≤ .05) cells. The clonogenic potential of the >4N fraction is
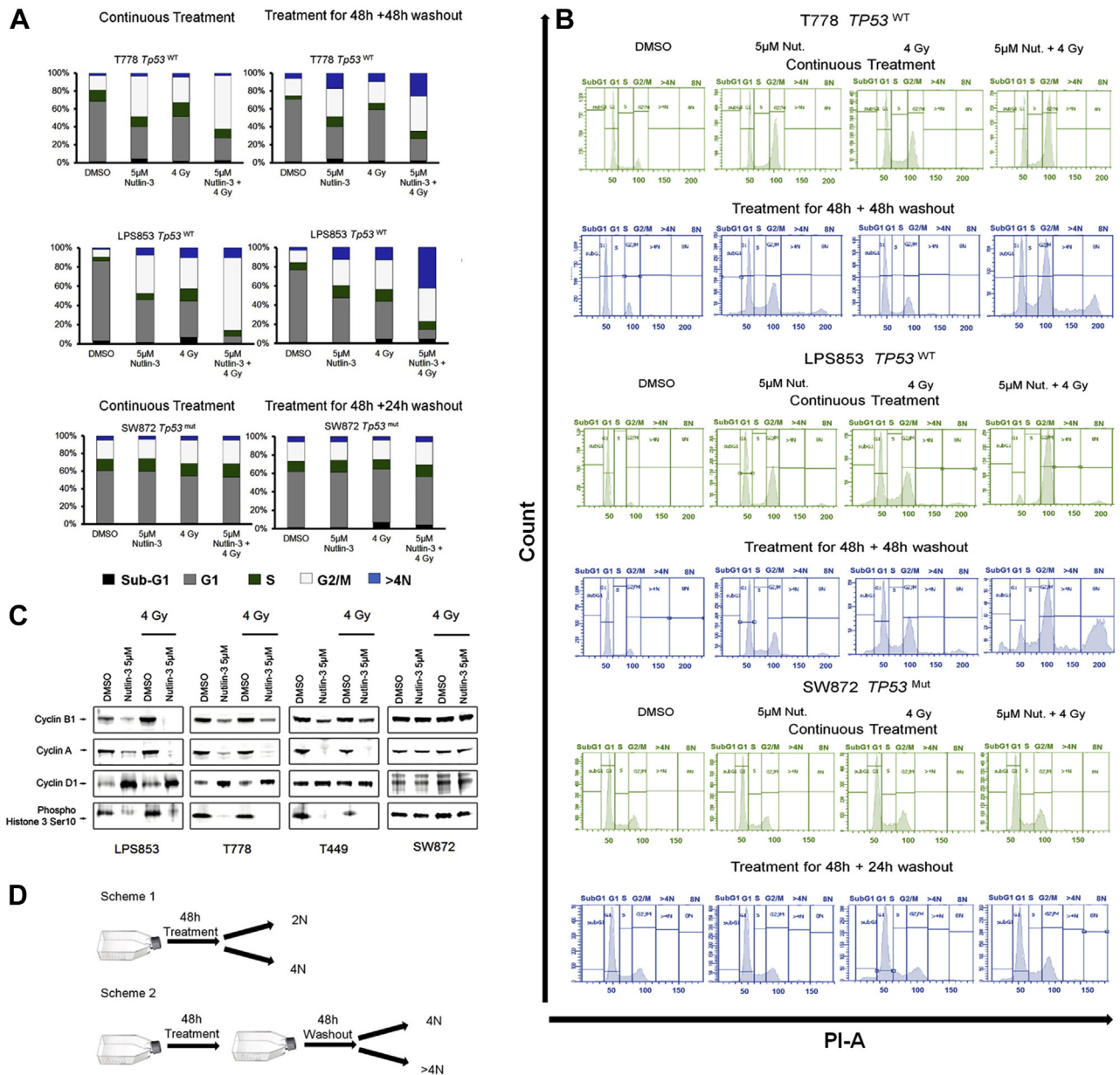
Figure 3 Perturbation in cell cycle progression markers and emergence of ploidy-based subpopulations in a p53-dependent way. (A) Fluorescence-activated cell sorting analysis of cell cycle distribution after 48 hours of treatment with or without washout in LPS853, T778, and SW872. (B) Histograms represent the corresponding DNA content. (C) Immunoblotting of cell cycle progression markers (cyclin A, cyclin D1, cyclin B1, phospho-histone H3 ser-10) in all cell lines after 48 hours of treatment. For β-actin stain, refer to Fig. 2. (D) Experimental scheme for sorting the 2N, 4N, and >4N populations by Hoechst 33342 stain.

almost completely impaired in response to RT alone and in the combination therapy (Fig 4A).

Discussion

MDM2 amplification and TP53 mutation are mutually exclusive in cancer and frequently observed in sarcomas.[19] Liposarcomas represent one of the most common sarcoma subtypes[20] and are known to harbor the amplified MDM2 with wild-type TP53.[21]

In preclinical models of laryngeal, lung, or prostate cancer, MDM2 inhibitors have yielded enhanced vulnerability of cancer cells to RT through diverse p53-dependent cell fate mechanisms such as cell cycle arrest, apoptosis, and senescence.[22-24] This is the first report of the potential mechanism by which MDM2 inhibitor and RT lead ultimately to a radiosensitization effect in a certain subset of TP53 wild-type sarcomas by shifting the ploidy-based heterogeneity, reducing clonal ability, and enhancing senescence of the polyploid cells.
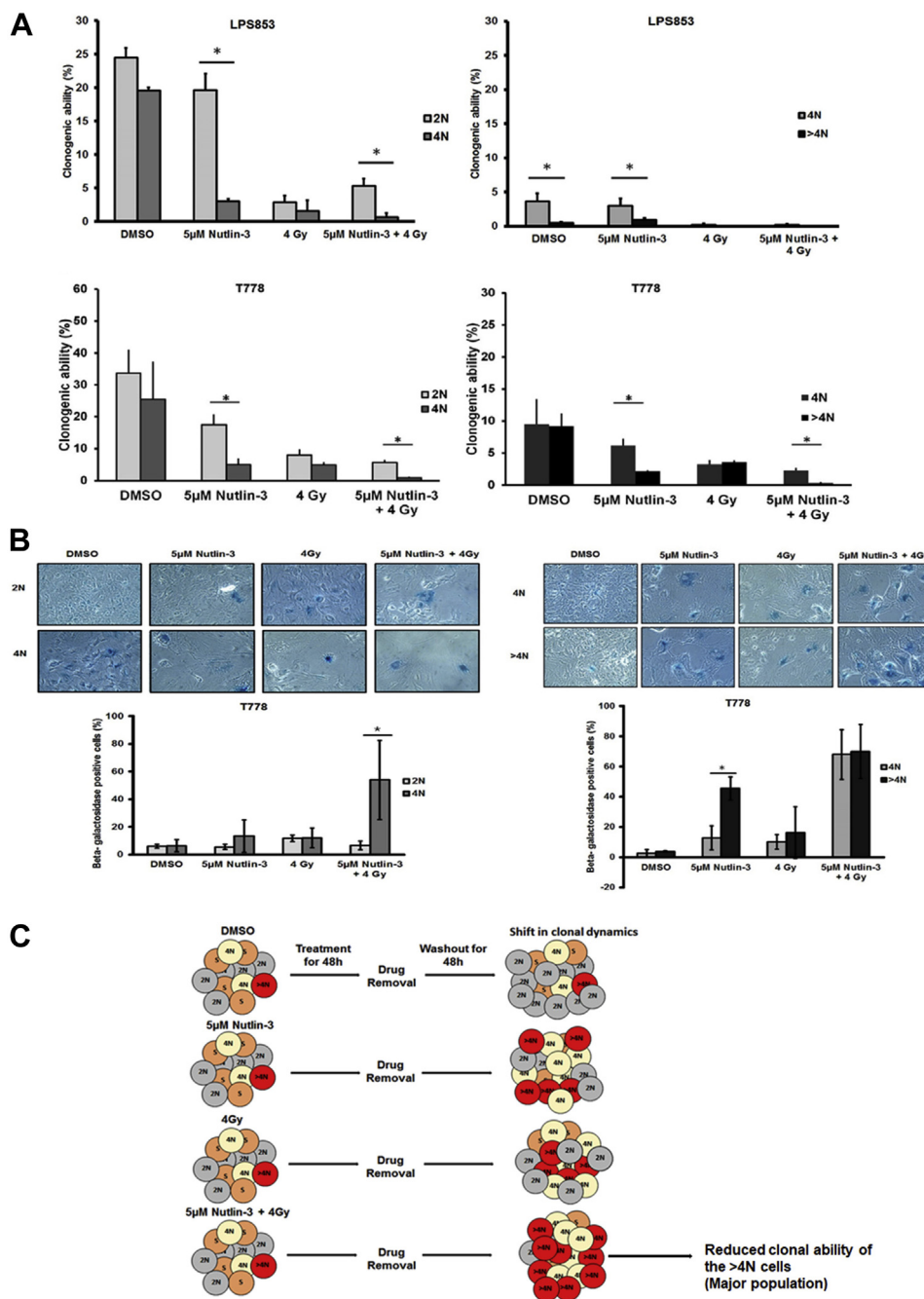
Figure 4 Long-term fate: combination therapy induces polyploid cells and impaires their colony forming ability in LPS853 and T778. (A) Colony assays for sorted 2N, 4N, and >4N populations following scheme 1 and scheme 2. Error bars represent ± standard deviation. (B) Senescence induction in sorted 2N, 4N, and >4N populations to assess long-term fate in T778. (C) Schematic representing the mechanism of shifting the clonal dynamics and impairment of clone forming ability of the polyploid population. *$P \leq .05$.

This study also revealed that the presence of wild-type *TP53* from a treatment perspective is essential but not the sole determinant of therapy-driven efficacies.

By clonogenic assays with 3 *TP53* wild-type cell lines (T778, LPS853, and T449), it was evident that SER was higher than 1 in 2 lines (T778 $SER_{10} = 1.3$ and LPS853 $SER_{10} = 1.4$), whereas the other displayed an antagonistic effect (T449 $SER_{10} = 0.79$). As expected, SW872

harboring *TP53* mutation ($SER_{10} = 1.02$) was not responsive to co-treatment, reinforcing the existing proof-of-concept for the requirement of functional *TP53* for responsiveness to nutlin-type drugs.

As observed in the present set of studies, short-term analysis of the cellular phenotypic fates driven by the therapies displayed cell cycle arrest at G2 and senescence. However, the cell cycle markers (G1, G2/M) were not

detected in congruence with the DNA content, and emergence of the 4N G1 cells was observed. Cell cycle analysis followed by drug removal revealed a shift in ploidy-based clonal heterogeneity (ie, dominance of 4N and >4N populations). Maki et al described this process as endo-reduplication[25] and as having a possible association with therapy resistance. However, there are several processes of polyploidy generation, such as cell fusion, abortive cell cycle (karyokinesis failure or cytokinesis failure), and endo-reduplication.[26] Polyploid cells generated through endo-reduplication and karyokinesis failure harbor a single nucleus, whereas cells that emerge via cell fusion or cytokinesis failure possess multiple nuclei. As in this study, the cells displayed multinucleated polyploid cells by DAPI stain (Fig E3A; available online at https://doi.org/10.1016/j.adro.2019.11.004), which excludes the possibility of processes such as endo-reduplication and karyokinesis failure. Thus, it is conceivable that the cells were generated either by cell fusion or via cytokinesis failure, which might direct the final fate of the polyploid cells in different way.

Clonogenic assays imply long-term fates. By sorting the ploidy-based clonal populations (2N, 4N, and >4N) after treatment and treatment removal (Fig 3D, scheme 1 and 2) and analyzing the long-term fates by colony assay and senescence measurement, this study found attenuated colony-forming ability and induction of senescence in the >4N cells (Fig 4) in response to the combination therapy in T778 and LPS853. Upon nutlin-3 treatment and removal, polyploid (4N and >4N) cells were also observed in T449 (Fig E1A and E1B; available online at https://doi.org/10.1016/j.adro.2019.11.004). However, in T449, the clonal ability of the 2N populations was observed to be higher than 4N populations. Clone-forming ability of >4N was substantially diminished by nutlin-3 alone. In contrast to the other cells (T778 and LPS853), RT treatment did not further enhance the effect in T449 (Fig E1C and E1D; available online at https://doi.org/10.1016/j.adro.2019.11.004). Induction of senescence was also not observed (Fig E1E and E1F; available online at https://doi.org/10.1016/j.adro.2019.11.004). Thus, wild-type TP53 was not the sole determinant of the ultimate fate in liposarcoma in response to RT and MDM2 inhibitors. The compensatory pathways might be responsible for determining the fate, which warrants further investigation. On a speculative note, aberrations of cell cycle proteins (eg, cyclin D1) were observed to be overexpressed in T449 (Fig 3C) and other LPS cell line LPS141 (Fig E2B; available online at https://doi.org/10.1016/j.adro.2019.11.004) and might be a determinant, which requires further validation.

SW872 did not show to induce therapy-driven polyploid populations on removal of nutlin-3. Thus, it is possible that generation of the polyploid cells upon nutlin-3 treatment (±RT) in the genetic background of liposarcoma is a p53-dependent phenomenon with diverse fates governed by multiple factors.

Immunoblotting of the MDM2-p53-p21 axis revealed enhanced reactivation of p53 in response to cotreatment. P53, in its turn, upregulated the expression of MDM2 via auto-regulatory loop.[27] As a downstream effect, p21 was induced by reactivated p53. The activation of the MDM2-p53-p21 axis in response to MDM2 inhibitors and RT was detected in other liposarcoma cell lines T449 (Fig 2B), LPS141 (Fig E2C; available online at https://doi.org/10.1016/j.adro.2019.11.004), and other sarcoma cell lines, such as GIST430 (gastrointestinal stromal tumors) and U2OS (osteosarcoma; Fig E4D; available online at https://doi.org/10.1016/j.adro.2019.11.004). However, these cell lines (T449 [Fig 2A-2D], LPS141 [Fig E2A; available online at https://doi.org/10.1016/j.adro.2019.11.004], and GIST430, U2OS [Fig E4A-C; available online at https://doi.org/10.1016/j.adro.2019.11.004]) did not show enhanced senescence or apoptosis in response to cotreatment despite harboring amplified MDM2 and wild-type TP53, which once again indicates the existence of compensatory regulatory pathways and that reactivation of wild-type p53 was not the sole determinant of the therapy-driven effect.

Conclusions

In synthesis, in the context of liposarcoma, it can be emphasized that disruption of MDM2-p53 interaction and reactivation of p53 by coapplication of MDM2 inhibitor and RT led to radiosensitization (SER greater than 1) as a long-term fate via attenuated clonal ability and senescence in the relatively abundant polyploid population (Fig 4C), which emerged either by cytokinesis failure or cell fusion. However, therapy-generated polyploid populations might have diverse fates governed by additional factors. This study indicated potential clinical translation in a subset of liposarcoma patients that warrants further investigation.

Acknowledgments

Supplementary data

Supplementary material for this article can be found at https://doi.org/10.1016/j.adro.2019.11.004.

References

1. Bieging KT, Mello SS, Attardi LD. Unravelling mechanisms of p53-mediated tumour suppression. *Nat Rev Cancer*. 2014;14:359-370.
2. Muller PA, Vousden KH. Mutant p53 in cancer: New functions and therapeutic opportunities. *Cancer Cell*. 2014;25:304-317.
3. Oren M, Rotter V. Mutant p53 gain-of-function in cancer. *Cold Spring Harb Perspect Biol*. 2010;2:a001107.
4. Oliner JD, Kinzler KW, Meltzer PS, George DL, Vogelstein B. Amplification of a gene encoding a p53-associated protein in human sarcomas. *Nature*. 1992;358:80-83.
5. Momand J, Jung D, Wilczynski S, Niland J. The MDM2 gene amplification database. *Nucleic Acids Res*. 1998;26:3453-3459.
6. Chene P. Inhibiting the p53-MDM2 interaction: An important target for cancer therapy. *Nature Reviews Cancer*. 2003;3:102-109.
7. Momand J, Zambetti GP, Olson DC, George D, Levine AJ. The mdm-2 oncogene product forms a complex with the p53 protein and inhibits p53-mediated transactivation. *Cell*. 1992;69:1237-1245.
8. Moll UM, Petrenko O. The MDM2-p53 interaction. *Mol Cancer Res*. 2003;1:1001-1008.
9. Tao WK, Levine AJ. Nucleocytoplasmic shuttling of oncoprotein Hdm2 is required for Hdm2-mediated degradation of p53. *P Natl Acad Sci USA*. 1999;96:3077-3080.
10. Coindre JM. [New WHO classification of tumours of soft tissue and bone]. *Ann Pathol*. 2012;32(5 Suppl):S115-S116.
11. Chibon F, Mariani O, Derre J, et al. A subgroup of malignant fibrous histiocytomas is associated with genetic changes similar to those of well-differentiated liposarcomas. *Cancer Genet Cytogen*. 2002;139:24-29.
12. Barretina J, Taylor BS, Banerji S, et al. Subtype-specific genomic alterations define new targets for soft-tissue sarcoma therapy. *Nat Genet*. 2010;42:715-721.
13. Coindre JM, Pedeutour F, Aurias A. Well-differentiated and dedifferentiated liposarcomas. *Virchows Arch*. 2010;456:167-179.
14. Oliner JD, Saiki AY, Caenepeel S. The role of MDM2 amplification and overexpression in tumorigenesis. *Cold Spring Harb Perspect Med*. 2016;6.
15. Shangary S, Wang S. Targeting the MDM2-p53 interaction for cancer therapy. *Clin Cancer Res*. 2008;14:5318-5324.
16. Wang S, Zhao Y, Aguilar A, Bernard D, Yang CY. Targeting the MDM2-p53 protein-protein interaction for new cancer therapy: Progress and challenges. *Cold Spring Harb Perspect Med*. 2017;7.
17. Duensing A, Medeiros F, McConarty B, et al. Mechanisms of oncogenic KIT signal transduction in primary gastrointestinal stromal tumors (GISTs). *Oncogene*. 2004;23:3999-4006.
18. Ou WB, Lu M, Eilers G, et al. Cotargeting of FAK and MDM2 triggers additive antiproliferative effects in mesothelioma via a coordinated reactivation of p53. *Br J Cancer*. 2016;115:1253-1263.
19. Leach FS, Tokino T, Meltzer P, et al. p53 Mutation and MDM2 amplification in human soft tissue sarcomas. *Cancer Res*. 1993;53(10 Suppl):2231-2234.
20. Dodd LG. Update on liposarcoma: A review for cytopathologists. *Diagn Cytopathol*. 2012;40:1122-1131.
21. Conyers R, Young S, Thomas DM. Liposarcoma: Molecular genetics and therapeutics. *Sarcoma*. 2011;2011:483154.
22. Arya AK, El-Fert A, Devling T, et al. Nutlin-3, the small-molecule inhibitor of MDM2, promotes senescence and radiosensitises laryngeal carcinoma cells harbouring wild-type p53. *Br J Cancer*. 2010;103:186-195.
23. Cao C, Shinohara ET, Subhawong TK, et al. Radiosensitization of lung cancer by nutlin, an inhibitor of murine double minute 2. *Mol Cancer Ther*. 2006;5:411-417.
24. Feng FY, Zhang Y, Kothari V, et al. MDM2 inhibition sensitizes prostate cancer cells to androgen ablation and radiotherapy in a p53-dependent manner. *Neoplasia*. 2016;18:213-222.
25. Shen H, Moran DM, Maki CG. Transient nutlin-3a treatment promotes endoreduplication and the generation of therapy-resistant tetraploid cells. *Cancer Res*. 2008;68:8260-8268.
26. Storchova Z, Pellman D. From polyploidy to aneuploidy, genome instability and cancer. *Nat Rev Mol Cell Biol*. 2004;5:45-54.
27. Wu X, Bayle JH, Olson D, Levine AJ. The p53-mdm-2 autoregulatory feedback loop. *Genes Dev*. 1993;7:1126-1132.